PCCP

ROYAL SOCIETY OF CHEMISTRY

PAPER

View Article Online
View Journal | View Issue

Cite this: *Phys. Chem. Chem. Phys.*, 2022, **24**, 10378

Probing the presence and absence of metal-fullerene electron transfer reactions in helium nanodroplets by deflection measurements†

John W. Niman, [a] Benjamin S. Kamerin, [a] Thomas H. Villers,[a] Thomas M. Linker,[b] Aiichiro Nakano[b] and Vitaly V. Kresin *[a]

Received 14th February 2022,
Accepted 12th April 2022

DOI: 10.1039/d2cp00751g

rsc.li/pccp

Metal-fullerene compounds are characterized by significant electron transfer to the fullerene cage, giving rise to an electric dipole moment. We use the method of electrostatic beam deflection to verify whether such reactions take place within superfluid helium nanodroplets between an embedded C_{60} molecule and either alkali (heliophobic) or rare-earth (heliophilic) atoms. The two cases lead to distinctly different outcomes: $C_{60}Na_n$ (n = 1–4) display no discernable dipole moment, while $C_{60}Yb$ is strongly polar. This suggests that the fullerene and small alkali clusters fail to form a charge-transfer bond in the helium matrix despite their strong van der Waals attraction. The $C_{60}Yb$ dipole moment, on the other hand, is in agreement with the value expected for an ionic complex.

1 Introduction

Since the discovery of alkali-doped fullerides and their superconductivity,[1,2] it has been known that metal atom-fullerene structures with significant charge transfer are readily formed in the bulk, surface,[3] and gas phases.[4–6] Gas-phase studies are informative because they permit a molecular-level analysis of the charge transfer process.

The formation of an ion pair implies the appearance of a large dipole moment, and indeed studies of fullerene-alkali systems by molecular beam electric deflection[7] have demonstrated high electric susceptibilities related to extremely large (~10–20 D) dipole moments in these systems. Interestingly, these experiments showed that at higher temperatures the alkali metal atoms and clusters appear to skate about the surface of the fullerene. Analogously, complexes of C_{60} with transition metals were found to have dipole moments of 6–10 D.[8]

Helium nanodroplet embedding offers a method to assemble and study such systems at very low temperatures and within a superfluid environment.[9] Rotational and vibrational motion are greatly suppressed at the nanodroplet temperature of 0.37 K, and polar complexes can be strongly oriented by an external electric field and interrogated by pendular spectroscopy[10,11] and electrostatic deflection.[12]

However, there is a hurdle: alkali atoms are strongly heliophobic and are not wetted by the helium medium.[13] As a result, alkali atoms and small clusters do not submerge into helium nanodroplets and instead reside in surface dimples.[14–17] On the other hand, recent work by Renzler *et al.*[18] provided evidence, based on electron ionization mass spectrometry, that co-doping helium nanodroplets with the highly polarizable C_{60} molecule induces Na atoms, as well as small clusters of Na and Cs, to submerge into the nanodroplet. It was suggested that this could derive from the strong long-range van der Waals attraction between the partners,[19] or from electron transfer *via* a harpoon reaction. A follow-up computational study[20] concluded that harpoon-type charge transfer may take place between Cs_2 and fullerene dopants.

The presence or absence of an ion pair within a nanodroplet can be directly established by the electrostatic deflection method. In this work we apply it to the sodium-C_{60} system and demonstrate that for $C_{60}Na_{n=1-4}$ there is in fact no evidence of a strong electric dipole appearing in the system, and hence of the partners approaching closely enough to form an ionic bond.

For a comparative measurement, we performed a deflection measurement for nanodroplets doped with C_{60} and ytterbium atoms. Yb was chosen due to the combination of a favorable ionization energy and vapor pressure. It is also pertinent that ytterbium-intercalated fulleride conductors have been synthesized[21] and were found to exhibit superconductivity. While to the best of our knowledge Yb previously has not been used as a nanodroplet dopant, it is unambiguously expected to

[a] *Department of Physics and Astronomy, University of Southern California, Los Angeles, CA 90089-0484, USA. E-mail: kresin@usc.edu*
[b] *Collaboratory for Advanced Computing and Simulations, University of Southern California, Los Angeles, CA 90089-0242, USA*

† Electronic supplementary information (ESI) available. See DOI: https://doi.org/10.1039/d2cp00751g

solvate, analogously to Eu, another rare-earth atom.[22] Here we observe a sizable deflection indicative of the formation of a large electric dipole. The magnitude of the dipole is in very good agreement with the computed dipole moment for a Yb atom positioned on a pentagonal face of the fullerene, implying that an electron is readily transferred and a bound $C_{60}Yb$ system is formed.

2 Experiment

As described in ref. 12 and 23, a supersonic beam of helium nanodroplets is generated by expansion of ultrahigh purity grade helium gas at 80 bar stagnation pressure through a 5 micron nozzle held at a temperature of 15 K. The beam is skimmed, and chopped by a rotating wheel; the beam velocity is measured to be $\approx$375 m s^{-1}. It then passes through two heated stainless steel pick-up cells, with the first containing C_{60} powder (99.9%) and the second a small lump of Na (99.99%, loaded under hexane to combat oxidation) or of Yb chips (99.95%). The dopants are picked up by sequential collisions with the droplet beam and their thermal energy is promptly dissipated by partial evaporation of the droplet.[9]

The pick-up process follows Poisson statistics. The cell temperatures were stabilized to optimize the signal to a desired average number of dopants. The temperature of C_{60} was fixed to a value between 370 °C and 380 °C. This yielded sufficient intensity in the mass spectrum at the single C_{60}^+ mass while keeping the intensity of the C_{60} dimer to a negligible level. (At this temperature many of the fullerene's vibrational modes[24] are activated, hence pick-up of one molecule results in the nanodroplet shrinking by $\sim$9000 He atoms.) Deflection measurements of $C_{60}Na_n$ were taken with the metal-containing cell temperature ranging from 190 °C to 210 °C, and of $C_{60}Yb$ with this cell at 360 °C.

The beam then travels to the deflection chamber where it is collimated by a 0.25 mm $\times$ 1.25 mm slit, and passes between two 15 cm-long high voltage electrodes which create an electric field and a collinear field gradient directed perpendicular to the beam axis. With an applied voltage of 20 kV, a field strength of 82 kV cm^{-1} with a gradient of 338 kV cm^{-2} is achieved.[25] The nanodroplets then traverse a 1.25 m free-flight region and enter the aperture of a quadrupole mass spectrometer (Ardara Technologies), where they are ionized by electron impact with an electron energy of 70 eV and detected using a pulse-counting channeltron multiplier with a digital counter system synchronized to the chopper.[26] With this arrangement, deflection profiles can be acquired even with counting rates as low as a few per second.

Among the peaks in the mass spectrum there are those which correspond to bare $C_{60}M^+$ ions, where *M* is a metal atom or cluster. These ions are ejected from the droplet following charge exchange with a He^+ hole generated by electron-impact ionization.[15] Note that they may derive either from post-ionization encounters between C_{60}^+ and M (or between C_{60} and M^+), or from the ionization of bound $C_{60}M$ complexes preformed in the nanodroplets. The aim of the measurement is to ascertain whether nanodroplets contain any polar complexes of the latter type, formed by a charge transfer reaction. It is worth reiterating that the deflection step occurs before ionization of the beam, and therefore the reactants and the complexes are electrically neutral.

Deflection profiles were collected by setting the mass spectrometer to these peaks and translating the detection chamber on a precision linear slide, controlled by a stepper motor, under two conditions: ''field-off'' and ''field-on.'' The former establishes the original cross section of the beam, and the latter determines the magnitude of beam deviation under the influence of the electric field. As mentioned above, the very low temperature of the helium nanodroplets allows for nearly complete orientation of the permanent dipole of the embedded dopant along the electric field. This permits the force from the electric field gradient on the dipole to become so strong as to deflect the entire heavy nanodroplet on the scale of millimeters.

The initial nanodroplet size distribution in the beam is calibrated by deflections using a dopant with a known dipole moment, in this case CsI. For the conditions employed in the present measurements, the mean size was found to be $\approx 2 \times 10^4$ helium atoms per droplet. Based on this information, we can solve for the dipole moment of a polar embedded complex by fitting its ''field-on'' profile to a Monte Carlo simulation of the deflection process. Using the ''field-off'' profile as input, it simulates the beam's path by accounting for the dopants' pick-up probabilities, post-pickup droplet shrinkage by evaporation, dipole orientation in the electric field region, a correction for the polarization of the helium matrix, the deflection angle induced by the field gradient, and finally the size dependence of the probabilities of droplet ionization and subsequent charge transfer to the dopant. This procedure is described in our previous publications.[12,23,27,28]

3 Results

3.1 Sodium

Fig. 1 displays the $C_{60}Na_n$ mass spectra over the temperature range used for deflection measurements. The peak widths are partially due to the presence of ^{13}C isotopes in the fullerene. Note that the ion signals are quite weak compared to the intensity of the bare fullerene peak. The $C_{60}Na^+$ signal is the weakest of all, including at cell temperatures outside of the range shown. Thus, sodium has a low propensity for forming bound complexes with C_{60}. To determine whether they ever establish direct contact as neutral dopants, we look for evidence of the formation of a dipole moment.

Electrostatic beam deflections were performed at the temperatures shown in Fig. 1. At these settings a given mass peak acquires sufficient intensity for a profile measurement, while the larger ones remain weak, minimizing the likelihood of their fragmentation contaminating the peak of interest. This strategy could not be adopted for $C_{60}Na$ due to its low peak intensity but was followed for $C_{60}Na_{2-4}$.

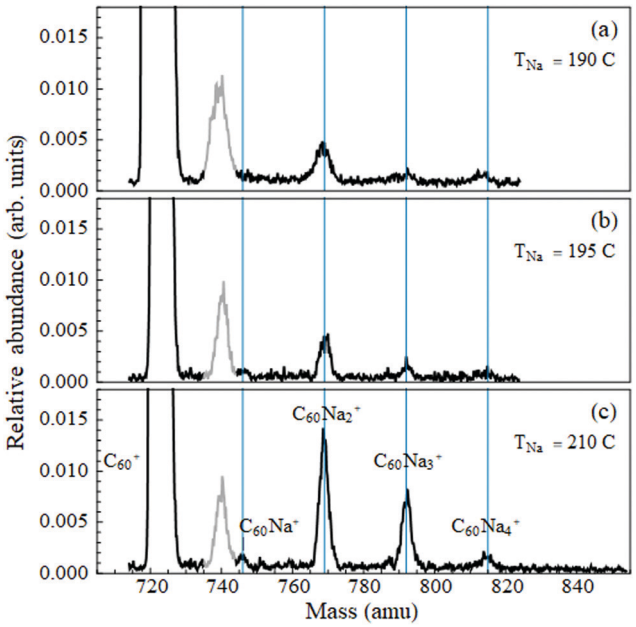

Fig. 1 Mass spectra of $C_{60}Na_n^+$ ions with the corresponding Na pick-up cell temperatures indicated. All spectra are normalized to the intensity of the C_{60}^+ peak. The $C_{60}Na^+$ signal is weak for all temperatures. The gray peak is the C_{60}-water complex. Panels (a) and (b) show the conditions used for deflection measurements of the $C_{60}Na_2^+$ and $C_{60}Na_3^+$ peaks, respectively, while (c) gives the conditions for $C_{60}Na^+$ and $C_{60}Na_4^+$ deflections.

Fig. 2 shows the undeflected and deflected beam profiles acquired with the mass spectrometer set to the $C_{60}Na_n^+$ peaks. For all measured n the deflection is essentially negligible within the accuracy of the measurement. This is in striking contrast with the 14–16 D dipole moment of the ionic $C_{60}Na$ molecule,[8,29] which would have resulted in deflections on the order of several millimeters,[30] and confirms that no charge-transfer bound complexes between the fullerene cluster and the sodium atom form within the nanodroplet.

Note that the average nanodroplet size in this work is approximately 25 times smaller than in ref. 18, and the average radius is therefore almost three times smaller[9] ($\approx$60 Å *vs.* $\approx$175 Å). It is evident that this decrease in separation does not facilitate a charge-transfer reaction.

3.2 Ytterbium

The case for fullerenes and Yb atoms is qualitatively different. This was already hinted at by the mass spectra, where the ratio of the $C_{60}Yb^+$:C_{60}^+ peak intensities was an order of magnitude higher than for $C_{60}Na_n^+$:C_{60}^+. (The $C_{60}Yb$ mass spectrum is shown in the ESI†). Deflection measurements made the distinction apparent. Fig. 3(a) shows the ''field-off'' and ''field-on'' profiles of the $C_{60}Yb$ mass peak. A very sizable deviation is immediately evident, in contrast with the results for sodium, and establishes that the embedded complex has a large permanent electric dipole moment.

Following the fitting procedure described in Section 2, we deduce the magnitude of this dipole moment. The deflecting

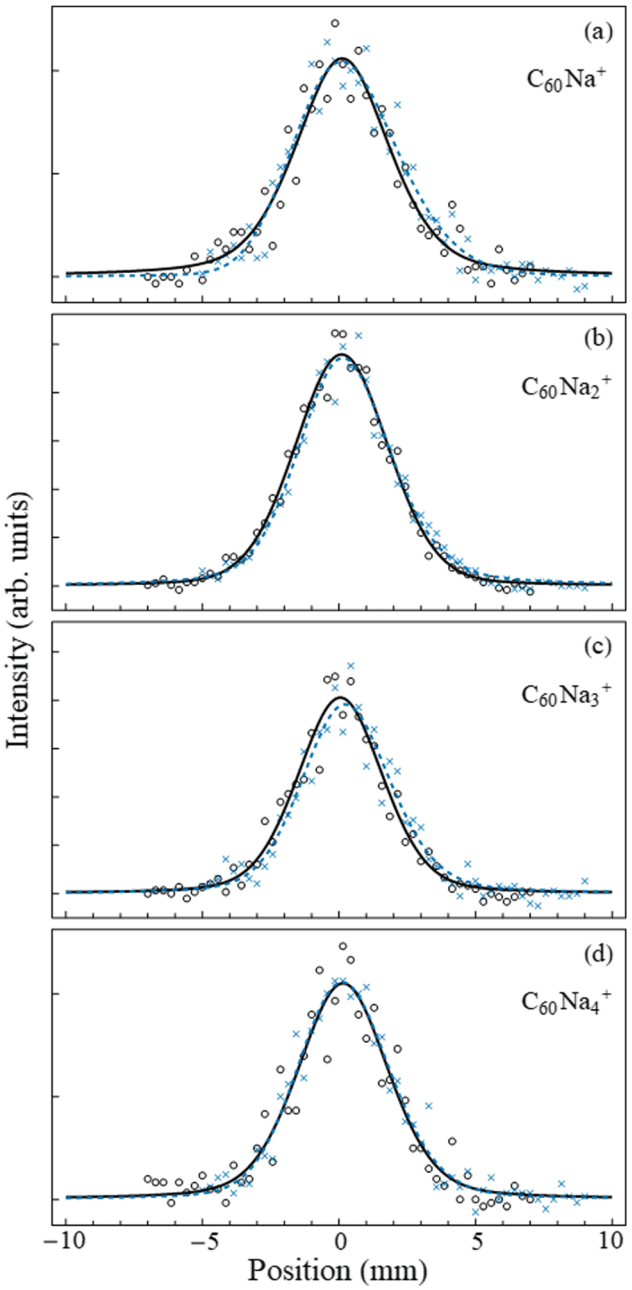

Fig. 2 Beam deflection measurements for nanodroplets containing $C_{60}Na_{n=1-4}$. Circles (crosses) denote data points with the electric field turned off (on). The counting rates of selected ions in the strongly collimated beam were on the order of a few per second. The solid-line profiles are smoothing fits to the ''field-off'' data points using a symmetric pseudo-Voigt function,[31] while the dashed lines are asymmetric pseudo-Voigt smoothing fits to the ''field-on'' data. In all cases the deflection is negligible.

force is proportional to the degree of orientation induced by the applied electric field onto the molecular dipole. Since the rotational constant of the $C_{60}Yb$ complex is small, it is accurate to use the classical Langevin-Debye expression for the orientation cosine.[32,33] Indeed, the fullerene rotational constant is[34] 0.003 cm^{-1} and that of the surface-bound Yb atom can be

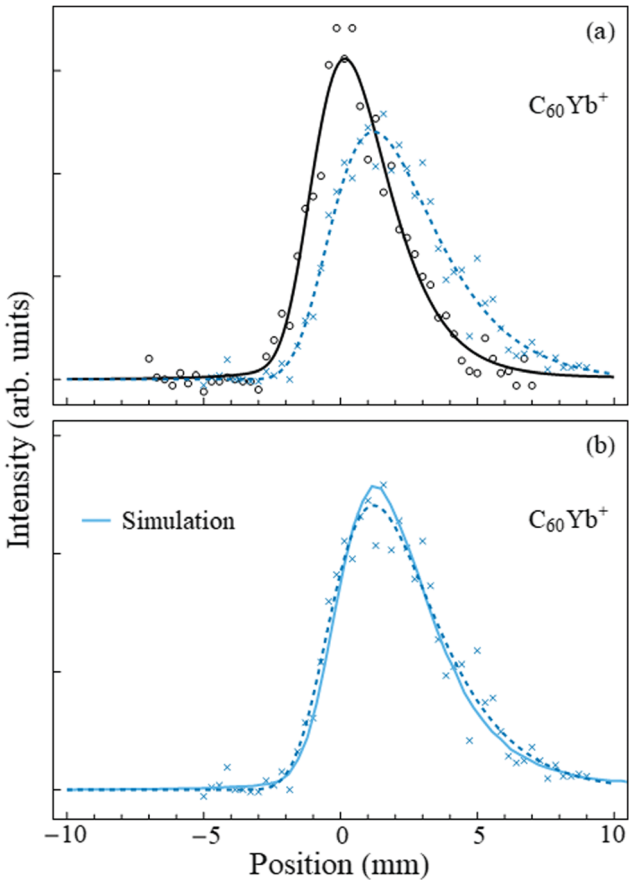

Fig. 3 Panel (a) shows the beam deflection measurements of nanodroplets containing $C_{60}Yb$ with the same notation as Fig. 2. A slight offset of the second pick-up cell added minor skewness to the profiles, hence in this figure both the "field-off" and the "field-on" data were fit to an asymmetric pseudo-Voigt profile. The shift of the profile centroid is ≈1.4 mm. Panel (b) shows the same "field-on" profile (dashed line) and data points, together with the Monte Carlo simulation (solid line) for the optimized dipole moment value of 8 D.

estimated by approximating its radial coordinate by the radius of C_{60}. The result for the complex is ≈ 0.024 cm^{-1} = 3.5 mK, which is two orders of magnitude lower than the nanodroplet temperature, and therefore many rotational states are occupied. For the given electric field strength, nanodroplet temperature, and the dipole moment quoted below, the orientation cosine is 0.98, *i.e.*, the complex becomes essentially completely oriented along the field.

Fig. 3(b) displays the result of the optimized fit and demonstrates good agreement with the experimental data. Based on this procedure we assign a dipole moment of 8 ± 1.5 D to the $C_{60}Yb$ complex. The estimated error bar, discussed in the ESI,† derives partially from the data fit and partially from the uncertainty in the branching ratio involved in the charge exchange between He^+ and the dopant.[12] The result unambiguously demonstrates that the rare earth metal atom contacts and donates charge to the fullerene.

As shown in the next section, the experimentally deduced value of the dipole moment is in good agreement with a calculation of the $C_{60}Yb$ complex, in particular for Yb atoms positioned at the pentagonal face of the fullerene. According to the computation, this situation has a marginally advantageous binding energy (although it is known that systems embedded in helium nanodroplets are not always able to reach their lowest energy geometries). Measurements of crystalline fullerene-ytterbium compounds suggest that the pentagonal face is indeed preferred for charge transfer,[35,36] supporting our results.

4 Calculations

To further validate the result for $C_{60}Yb$, the dipole moments and binding energies of free-space molecules were computed by plane-wave based Density Functional Theory (DFT). Calculations were performed in the Vienna *Ab Initio* Software Package (VASP).[37,38] Electronic states were computed within the frozen core approximation using the projected augmented wave-vector (PAW) method[39,40] with projectors generated for the C 2s and 2p states and the Yb 6s and 5p states. The strongly correlated Yb f electrons were assumed not to be involved in bonding and were kept within the core of the pseudopotential. A plane wave cut-off energy of 500 eV and the Perdew–Burke–Ernzerhof (PBE)[41] styled generalized gradient approximation (GGA) for the exchange–correlation functional were used. The C_{60} and $C_{60}Yb$ molecules were placed in the center of a non-cubic 15 Å × 18 Å × 20 Å box to remove spurious image interactions. Optimization was first performed on the C_{60} molecule to obtain its ground state structure. For computation of the binding energies and dipole moment the ground state C_{60} structure was kept frozen during the optimization of $C_{60}Yb$. Linear dipole corrections were used to correct the errors introduced by the periodic boundary conditions.[42]

The results of these calculations are presented in Table 1 alongside similar ones for the dipole moment of isolated $C_{60}Na$. The latter are in reasonable agreement with previous computations[29] and partially validate the present results for $C_{60}Yb$. As mentioned in the preceding section, it is found that settling the Yb atom on the pentagonal face yields a marginally higher binding energy and a noticeably lower dipole moment.

5 Summary

The experiments detect no sizable electric dipole moment appearing when a fullerene molecule, followed by between one and several sodium atoms, is embedded in helium nanodroplets. Therefore

Table 1 DFT calculations for the dipole moment and binding energy of a Yb or Na atom optimized on either the hexagonal or pentagonal face of the C_{60} fullerene

	Dipole moment (D)		Binding energy (eV)	
	Pentagon	Hexagon	Pentagon	Hexagon
$C_{60}Yb$	8.5	13.0	0.58	0.54
$C_{60}Na$	13.4	12.8	1.16	1.21

even if a heliophobic alkali atom is pulled inside the nanodroplet by the presence of C_{60},[18] it appears that they continue to be separated by a helium barrier and neither short-range electron transfer nor a longer-range harpoon reaction takes place.

The measurement does not provide information about the size of this separation barrier, and therefore an interesting question for further theoretical and experimental analysis is whether the Na atom and C_{60} form a weakly bound van der Waals-type complex, and how far apart they remain.

As for the absence of an electric dipole moment for $C_{60}Na_{2-4}$, one can envision two scenarios. One is that the sequentially picked up atoms assemble into a small sodium cluster on or near the droplet surface but still fail to approach the fullerene within the droplet sufficiently to transfer charge and form a bond. This contrasts with $C_{60}Na_n$ agglomerates forming in neat molecular beams.[43] An alternative possibility is that multiple sodium atoms do attach to the fullerene but arrange themselves in symmetric configurations, as calculated for lowest-energy structures due to Coulomb repulsion between positive sodium ions.[29] This cannot be excluded, but would require either a sequence of individual atom-C_{60} agglomeration events (which appear unlikely within the nanodroplets in view of the data), or attachment of a Na cluster followed by its separation into individual atoms and their subsequent rearrangement around the cage (which, however, would need to proceed in the very low-temperature nanodroplet environment). Consequently, the data do not support the theoretical picture[20] of an alkali dimer undergoing a harpoon reaction with C_{60} and settling into an ionic arrangement with the latter.

In contrast to sodium, we observe that a very strong permanent dipole moment is formed between ytterbium atoms (which are wetted by helium) and C_{60}, revealing successful electron transfer and bond formation in this system. Comparison with modeling of the $C_{60}Yb$ molecule suggests that the ytterbium atom prefers to locate above the pentagonal face of the fullerene. Interestingly, while the harpoon reaction is suppressed in binary collisions in the gas phase[19] due to unfavorable Franck–Condon factors,[44] in the present case the strong reactive channel is kept open thanks to removal of the accompanying vibrational excitation by the helium matrix.

It would be interesting to extend such measurements to larger alkali clusters, because above a certain critical size they begin to submerge into the nanodroplet by themselves.[45,46] This should promote charge transfer and dipole formation, analogous to observations on C_{60}-alkali cluster complexes in free space.[7] Interesting complementary information also could be derived from spectroscopic experiments, since near-IR absorption peaks of the fullerenes have been shown[47] to be sensitive to the oxidation state of C_{60}^{n-}.

Conflicts of interest

There are no conflicts to declare.

Acknowledgements

We would like to express our appreciation to Prof. G. Benedek for his eminent contributions to research on helium nanodroplets, fullerenes, and nanoclusters. We would like to thank L. Kranabetter and P. Scheier for productive discussions and R. E. Pedder for advice on sensitivity calibration of the quadrupole mass spectrometer. The research of J. W. N, B. S. K., T. H. V. and V. V. K. was supported by the U. S. National Science Foundation, Division of Chemistry under Grants No. CHE-1664601 and CHE-2153255. T. M. L. and A. N. were supported by the National Science Foundation, Award OAC-2118061. Simulations were performed at the Center for Advanced Research Computing of the University of Southern California. The figures for this article were generated using the SciDraw scientific figure preparation system.[48]

References

1 A. F. Hebard, *Annu. Rev. Mater. Sci.*, 1993, **23**, 159–191.
2 O. Gunnarsson, *Alkali-Doped Fullerides: Narrow-Band Solids with Unusual Properties*, World Scientific, Singapore, 2004.
3 M. R. C. Hunt, S. Modesti, P. Rudolf and R. E. Palmer, *Phys. Rev. B: Condens. Matter Mater. Phys.*, 1995, **51**, 10039.
4 L. S. Wang, O. Cheshnovsky, R. E. Smalley, J. P. Carpenter and S. J. Hwu, *J. Chem. Phys.*, 1992, **96**, 4028.
5 T. P. Martin, N. Malinowski, U. Zimmermann, U. Näher and H. Schaber, *J. Chem. Phys.*, 1993, **99**, 4210.
6 M. Pellarin, E. Cottancin, J. Lermé, J. L. Vialle, M. Broyer, F. Tournus, B. Masenelli and P. Mélinon, *Eur. Phys. J. D*, 2003, **25**, 31–40.
7 M. Broyer, R. Antoine, I. Compagnon, D. Rayane and P. Dugourd, *Phys. Scr.*, 2007, **76**, C135.
8 D. Rayane, A. R. Allouche, R. Antoine, I. Compagnon, M. Broyer and P. Dugourd, *Eur. Phys. J. D*, 2003, **24**, 9–13.
9 J. P. Toennies and A. F. Vilesov, *Angew. Chem., Int. Ed.*, 2004, **43**, 2622–2648.
10 M. Y. Choi, G. E. Douberly, T. M. Falconer, W. K. Lewis, C. M. Lindsay, J. M. Merritt, P. L. Stiles and R. E. Miller, *Int. Rev. Phys. Chem.*, 2006, **25**, 15–75.
11 D. Verma, R. M. P. Tanyag, S. M. O. O'Connell and A. F. Vilesov, *Adv. Phys.: X*, 2019, **4**, 1553569.
12 J. W. Niman, B. S. Kamerin, D. J. Merthe, L. Kranabetter and V. V. Kresin, *Phys. Rev. Lett.*, 2019, **123**, 043203.
13 F. Ancilotto, E. Cheng, M. W. Cole and F. Tiogo, *Z. Phys. B: Condens. Matter*, 1995, **98**, 323–329.
14 J. Tiggesbäumker and F. Stienkemeier, *Phys. Chem. Chem. Phys.*, 2007, **9**, 4748–4770.
15 A. Mauracher, O. Echt, A. M. Ellis, S. Yang, D. K. Bohme, J. Postler, A. Kaiser, S. Denifl and P. Scheier, *Phys. Rep.*, 2018, **751**, 1–90.
16 F. Stienkemeier and K. K. Lehmann, *J. Phys. B: At., Mol. Opt. Phys.*, 2006, **39**, R127.
17 C. Callegari and W. E. Ernst, Helium Droplets as Nanocryostats for Molecular Spectroscopy – from the Vacuum Ultraviolet to the Microwave Regime, in *Handbook of High Resolution Spectroscopy*, ed. M. Quack and F. Merkt, John Wiley & Sons, Chichester, 2011, vol. 1, pp. 1551–1594.

18 M. Renzler, M. Daxner, L. Kranabetter, A. Kaiser, A. W. Hauser, W. E. Ernst, A. Lindinger, R. Zillich, P. Scheier and A. M. Ellis, *J. Chem. Phys.*, 2016, **145**, 181101.
19 V. V. Kresin, V. Kasperovich, G. Tikhonov and K. Wong, *Phys. Rev. A: At., Mol., Opt. Phys.*, 1997, **57**, 383–387.
20 M. P. de Lara-Castells, A. W. Hauser and O. Mitrushchenkov, *J. Phys. Chem. Lett.*, 2017, **8**, 4284–4288.
21 E. Özdaş, A. R. Kortan, N. Kopylov, A. P. Ramirez, T. Siegrist, K. M. Rabe, H. E. Bair, S. Schuppler and P. H. Citrin, *Nature*, 1995, **375**, 126–129.
22 A. Bartelt, J. D. Close, F. Federmann, K. Hoffmann, N. Quaas and J. P. Toennies, *Z. Phys. D: At., Mol. Clusters*, 1997, **39**, 1–2.
23 D. J. Merthe and V. V. Kresin, *J. Phys. Chem. Lett.*, 2016, **7**, 4879–4883.
24 J. Menéndez and J. B. Page, Vibrational Spectroscopy of C_{60}, in *Light Scattering in Solids VIII*, ed. M. Cardona and G. Güntherodt, Springer; Berlin, 2006, 1, 27–95.
25 G. Tikhonov, K. Wong, V. Kasperovich and V. V. Kresin, *Rev. Sci. Instrum.*, 2002, **73**, 1204–1211.
26 N. Guggemos, P. Slavíček and V. V. Kresin, *Phys. Rev. Lett.*, 2015, **114**, 043401.
27 J. W. Niman, B. S. Kamerin, L. Kranabetter, D. J. Merthe, J. Suchan, P. Slavíček and V. V. Kresin, *Phys. Chem. Chem. Phys.*, 2019, **21**, 20764–20769.
28 B. S. Kamerin, J. W. Niman and V. V. Kresin, *J. Chem. Phys.*, 2020, **153**, 081101.
29 J. Roques, F. Calvo, F. Spiegelman and C. Mijoule, *Phys. Rev. B: Condens. Matter Mater. Phys.*, 2003, **68**, 205412.
30 While Fig. 1 shows that water, which is a ubiquitous contaminant in vacuum systems, is also present in the beam, the fact that there are no noticeable $C_{60}Na_nH_2O$ peaks indicates that the deflection profiles are uncontaminated. Furthermore, even the adsorption of a water molecule would not be able to extinguish such a big dipole moment.
31 A. L. Stancik and E. B. Brauns, *Vib. Spectrosc.*, 2008, **47**, 66–69.
32 B. Friedrich and D. Herschbach, *Int. Rev. Phys. Chem.*, 1996, **15**, 325–344.
33 J. Bulthuis, J. A. Becker, R. Moro and V. V. Kresin, *J. Chem. Phys.*, 2008, **129**, 024101.
34 P. B. Changala, M. L. Weichman, K. F. Lee, M. E. Fermann and J. Ye, *Science*, 2019, **363**, 49–54.
35 P. H. Citrin, E. Özdaş, S. Schuppler, A. R. Kortan and K. B. Lyons, *Phys. Rev. B: Condens. Matter Mater. Phys.*, 1997, **56**, 5213–5227.
36 X. Cao, Y. Wang, J. Hao, J. Liu, S. Hu and G. Lan, *J. Raman Spectrosc.*, 2000, **31**, 461–463.
37 G. Kresse and J. Hafner, *Phys. Rev. B: Condens. Matter Mater. Phys.*, 1993, **47**, 558(R).
38 G. Kresse and J. Furthmüller, *Phys. Rev. B: Condens. Matter Mater. Phys.*, 1996, **54**, 11169.
39 P. E. Blöchl, *Phys. Rev. B: Condens. Matter Mater. Phys.*, 1994, **50**, 17953.
40 G. Kresse and D. Joubert, *Phys. Rev. B: Condens. Matter Mater. Phys.*, 1999, **59**, 1758–1775.
41 J. P. Perdew, K. Burke and M. Ernzerhof, *Phys. Rev. Lett.*, 1996, **77**, 3865.
42 J. Neugebauer and M. Scheffler, *Phys. Rev. B: Condens. Matter Mater. Phys.*, 1992, **46**, 16067.
43 P. Dugourd, R. Antoine, D. Rayane, I. Compagnon and M. Broyer, *J. Chem. Phys.*, 2001, **114**, 1970–1973.
44 V. V. Kresin and V. Z. Kresin, *Z. Phys. D: At., Mol. Clusters*, 1997, **40**, 381–384.
45 C. Stark and V. V. Kresin, *Phys. Rev. B: Condens. Matter Mater. Phys.*, 2010, **81**, 085401.
46 L. An der Lan, P. Bartl, C. Leidlmair, H. Schöbel, R. Jochum, S. Denifl, T. D. Märk, A. M. Ellis and P. Scheier, *J. Chem. Phys.*, 2011, **135**, 044309.
47 D. R. Lawson, D. L. Feldheim, C. A. Foss, P. K. Dorhout, C. M. Elliott, C. R. Martin and B. Parkinson, *J. Electrochem. Soc.*, 1992, **139**, L68–L71.
48 M. A. Caprio, *Comput. Phys. Commun.*, 2005, **171**, 107–118.